Rhizosphere 37 (2026) 101294

Contents lists available at ScienceDirect

Rhizosphere

journal homepage: www.elsevier.com/locate/rhisph

Model-based insights on the relationship between planar root length density observed in minirhizotron images and volumetric root length density in the field

Magdalena Landl *, Sibghat Ullah, Lena Lärm, Anja Klotzsche, Jan Vanderborght, Andrea Schnepf

Forschungszentrum Juelich GmbH, Agrosphere(IBG-3), Juelich, Germany

ARTICLE INFO

Keywords:
Minirhizotron
Root length density
Root images
Root architecture model
CPlantBox

ABSTRACT

Minirhizotrons (MR) enable non-destructive investigation of plant root systems in the field. However, MR images only provide information about root systems in the 2D plane, whose relationship to 3D root system measures remains unclear. This study uses model simulation to investigate the relationship between planar root length density (pRLD) as determined from MR images and volumetric root length density (vRLD) in the field.

We set up a virtual MR facility resembling the field MR facilities in Selhausen. Root systems of maize and winter wheat were grown around horizontally laid rhizotubes in a virtual field setup using the root architecture model CPlantBox. We calculated pRLD from virtual MR images, as well as vRLD from virtual soil layers.

Our simulations confirmed experimental observations of weak correlations between pRLD and vRLD in topsoil, and of strong correlations in subsoil. The ratio of vRLD to pRLD remained relatively constant across the entire subsoil depth. The greater the heterogeneity in the distribution of root length density or in the anisotropy of root growth across depth, the higher the ratio of vRLD to pRLD. Different numbers of MR images led to similar mean pRLD values if the MR images were distributed evenly along the rhizotube length. Larger rhizotube diameters resulted in lower vRLD-to-pRLD ratios, while different plant densities had no effect.

Model simulation provides valuable insights into the factors influencing the relationship between pRLD and vRLD. It also draws attention to the potential and limitations of using minirhizotron image data, making it a useful complement to experimental studies.

1. Introduction

The ability of a plant to take up water and nutrients from the soil is largely determined by the structure of its root system. Knowledge of the size and distribution of root systems in the soil is therefore crucial for optimizing plants in terms of efficient water and nutrient utilization, drought resistance, and optimal yields. However, due to the opaque nature of the soil, it is difficult to examine root systems in the field. One well-established method for the non-destructive investigation of plant root systems in the field are minirhizotrons (MR), which consist of transparent tubes that are buried in the soil and in which images of roots growing along the tubes can be taken (Johnson et al., 2001; Box Jr. and Ramsuer, 1993; Heeraman and Juma, 1993; Vos and Groenwold, 1987). While it used to be a labor-intensive and time-consuming task to analyze such images (Cai et al., 2016; Garré et al., 2011), recent advances in deep learning approaches have enabled the processing of a large number of images with minimal user intervention and the automatic segmentation of roots from the image background (Bauer et al., 2022; Smith et al., 2020; Khoroshevsky et al., 2024). For this reason, the use of MR systems to study root systems in the field is experiencing a new renaissance 40 years after their invention with many recent publications (e.g. Böske et al. (2025), Holder et al. (2025), Black et al. (2017) and Lärm et al. (2024)).

One of the most frequently used root traits from MR studies is the root length density in a given soil volume, i.e., the volumetric root length density (vRLD) (Holder et al., 2025; Cai et al., 2018; Garré et al., 2011; Haarhoff et al., 2021; Geng et al., 2023). However, MR images as 2D windows into the soil only show root length per image area, i.e. the

This article is part of a special issue entitled: 10th anniversary_invited only published in Rhizosphere.

* Corresponding author. Forschungszentrum Juelich GmbH, Agrosphere (IBG-3) D- 52428 Juelich, Germany.
E-mail address: m.landl@fz-juelich.de (M. Landl).

https://doi.org/10.1016/j.rhisph.2026.101294
Received 5 December 2025; Received in revised form 13 February 2026; Accepted 15 February 2026
Available online 16 February 2026

planar root length density (pRLD) (Wacker et al., 2024). Various studies have raised doubts as to whether pRLD can be used to make meaningful statements about vRLD (Wacker et al., 2024; Bernier and Robitaille, 2004; Rytter and Rytter, 2012). Differences in soil texture, plant species, environmental conditions or soil depth may lead to variations in the relationship between pRLD and vRLD (Wacker et al., 2024). Furthermore, because of the heterogeneity of the soil and the stochastic nature of root systems, many MR images are required to obtain reliable pRLD values. Despite these doubts, numerous studies have found strong correlations between root length derived from MR images and vRLD from soil cores for different plant species including wheat (Arnhold et al., 2024; Box Jr. and Ramsuer, 1993; Ephrath et al., 1999), barley and faba bean (Heeraman and Juma, 1993), potato and field bean (Vos and Groenwold, 1987), cauliflower (Kage et al., 2000), maize (Liao et al., 2015; Samson and Sinclair, 1994) and tomato (Machado and Oliveira, 2003). It can therefore be assumed that the relationship between pRLD and vRLD varies depending on genetic and environmental factors as well as on the specifications of the MR system and the imaging procedure, but it is not yet clear in what way.

Different genetic and environmental conditions influence the geometric properties of root systems, which can be characterized by systematic trends, anisotropy of root growth, and root clustering (Grabarnik et al., 1998; Logsdon and Allmaras, 1991; Bengough et al., 2000; Tardieu, 1988). Systematic trends describe variations in root length density on a scale ranging from the root system to the field and are expected to influence the relationship between pRLD and vRLD, as variations in root length density will lead to different probabilities of a root being detected on an MR image. Root growth anisotropy describes a non-uniform orientation of roots in different directions and may give a bias to the root length detected on MR images (Baldwin et al., 1971; Lang and Melhuish, 1970). Root clustering defines the grouping of roots in the soil due to root branching and the location of plant rows on the scale of a few cubic centimeters and influences the relationship between pRLD and vRLD if the proportion of root clusters detected on MR images is not equal to the proportion of root clusters present in the soil (Tardieu, 1988; Logsdon and Allmaras, 1991).

Direct measurement of volumetric root measures in the field is limited to soil cores or soil monoliths, which represent only a small part of the root system and are not necessarily representative of the ground truth values within an entire soil layer (Morandage et al., 2019; Buczko et al., 2009). Furthermore, field measurements are limited to a specific experiment with a given setup of the MR system and the imaging procedure. Simulation models that describe root system architecture in 3D and allow for many replicates can thereby help to get a better insight into the relationship between pRLD and vRLD for a wide range of scenarios with different plant species and MR imaging specifications.

A prerequisite for model studies of minirhizotron systems is thereby the correct simulation of the growth direction of a root that encounters a rhizotube. Experimental studies have shown that the growth behavior of a root that encounters a rigid object represents a compromise between gravitropic and thigmotropic responses (Massa and Gilroy, 2003; Monshausen and Gilroy, 2009; Lee et al., 2020; Yao et al., 2024). The root system architecture model CPlantBox (Schnepf et al., 2018; Giraud et al., 2023) mimics this growth behavior by optimizing the growth direction of a new root segment for gravitropism and growth along the rigid object in a stochastic process.

In this study, we used the root system architecture model CPlantBox to simulate the growth of maize and winter wheat root systems in a virtual MR facility with horizontal rhizotubes resembling the field MR facilities in Selhausen (Lärm et al., 2023). We extracted pRLD from virtual MR images and vRLD from entire virtual soil layers. We ran simulation scenarios with various axial gravitropism parameterizations to account for environmental factors influencing the growth trajectories and determined the geometric properties of the simulated root systems, including systematic trends, root growth anisotropy, and root clustering. We analyzed the relationship between pRLD and vRLD at different depth levels as well as the influence of geometric properties on this relationship. Additionally, we ran simulation scenarios with different MR image sampling procedures, MR image sizes, rhizotube diameters, plant densities and soil sampling schemes and analyzed the influence of these factors on the relationship between pRLD and vRLD.

2. Material and methods

2.1. Virtual field setup

The virtual field setup aimed to reproduce the setup of the MR facilities Selhausen with the field experiment conducted in 2020 and 2021. A detailed description of the field experiment is given in Lärm et al. (2023). In short, the experimental test site in Selhausen consists of two MR facilities. The soil at the upper facility consists of a gravely, partly stony, and silty sand, whereas the soil at the lower facility consists of silty, sandy, and slightly gravely loam with significant clay content (Lärm et al., 2023). Each facility is divided into three plots, on which different varieties or mixtures of varieties of the plant species maize (2020) and winter wheat (2021) were grown.

2.1.1. Simulation of root system architecture in a field setup

We used the functional-structural plant model CPlantBox (Schnepf et al., 2018; Giraud et al., 2023) to simulate three-dimensional root systems of maize and winter wheat for full vegetation periods (120 days for maize and 215 days for winter wheat). CPlantBox distinguishes between different root types, i.e. tap root, basal roots and lateral roots of different order. Each root type is defined by a set of parameters that describe its development over time. To account for the stochasticity of the simulated root systems, all parameters are described by mean values and standard deviations. For the simulation of maize and winter wheat root architectures, we used the parameter sets given by Postma and Lynch (2011) and Morandage et al. (2019), respectively. In the maize root parameter set by Postma and Lynch (2011), the standard deviation of the root architecture parameters is generally set at 10% of the respective mean value. In contrast, the standard deviation of root architecture parameters in the winter wheat root parameter set by Morandage et al. (2019) ranges from 20% to 140% of the respective mean value. In accordance with Morandage et al. (2021), the parameter set of Morandage et al. (2019) was adapted so that the basal roots emerged at intervals of 9 days and not all at once. Seeding depths were set to 3 cm for both maize and winter wheat. To mimic a field setup, we simulated multiple plants with defined inter-row and inter-plant distance. For the maize crop, we simulated 6 rows with 8 maize plants within each row. In agreement with Lärm et al. (2023), the inter-row spacing was set to 75 cm, the inter-plant spacing to 12 cm, resulting in approximately 11 plants m^{-2}. For the winter wheat crop, we simulated 10 rows with 50 wheat plants within each row. The inter-row spacing was set to 21 cm, the inter-plant spacing to 1.5 cm, resulting in approximately 317 plants m^{-2} (Lärm et al., 2023). For each plant species, we performed 100 realizations of root system architecture simulations to account for model stochasticity.

2.1.2. Impact of environmental factors on root system architecture

Because our simulations do not consider environmental factors influencing the growth trajectories of individual roots, such as different soil types, bulk densities, and stone contents, the appearance of the simulated root architectures solely depends on the underlying root system parameters. However, since the tropism strength of axial roots is an important factor for the shape of a root system and its growth trajectories (Morris et al., 2017), we simulated root systems with a range of different gravitropism parameters for the axial roots instead of explicitly considering environmental influences on root growth. Specifically, we used 4 values from 1 to 4 for the CPlantBox parameter *tropismN*, which describes the strength of gravitropism and 8 values from 0.025 to 0.2 for the CPlantBox parameter *tropismS*, which describes the standard deviation of the random angular change in radians (Schnepf et al., 2018). In

this way, we obtained root system architectures with 32 different parameterizations of axial gravitropism for each plant species, which should cover possible changes in root system architecture due to environmental factors. A visualization of example realizations of root system architectures with the 32 different parameterizations of axial gravitropism for both maize and winter wheat is presented in Fig. S1 in the supplementary information.

2.1.3. Simulation of the growth direction of roots encountering rhizotubes

The horizontal rhizotubes of the MR facility act as obstacles to root growth. In CPlantBox, the geometry of rhizotubes is simulated explicitly using signed distance functions. The growth direction of a root that encounters a rhizotube is computed as follows: The axial and radial angles of a newly formed root segment are selected according to the gravitropically directed changes in growth direction using the values of *tropismN* and *tropismS* given in section 2.1.2. Using signed distance functions, the CPlantBox algorithm then checks whether the position of the root tip specified by the axial and radial angles is inside or outside the boundaries of the rhizotube. If the position is inside the rhizotube, a new pair of axial and radial angles is selected. First, a certain number of radial angles is selected at random, and the algorithm checks again whether any of the new pairs of axial and radial angles allow the root tip to be located outside the rhizotube. If this is not the case, the axial angle is increased by a small increment and the process of selecting a new number of radial angles is restarted. This approach makes it possible to simulate the experimentally observed growth behavior of a root that encounters a rhizotube, which represents a compromise between gravitropism and thigmotropism (Massa and Gilroy, 2003; Monshausen and Gilroy, 2009; Lee et al., 2020; Yao et al., 2024). To demonstrate the ability of CPlantBox in accurately simulating root growth around rhizotubes (i.e. circular obstacles), we conducted a simulation experiment based on a laboratory study by Yao et al. (2024). In this experiment, a maize seedling was allowed to grow around circular objects with a radius of 0.5 cm, which were arranged at regular intervals in a rhizobox of 1 cm depth that had a transparent front plate and was filled with agarose gel. The experimentally observed and simulated growth trajectories of the maize seedling are shown in Fig. S2 in the supplementary information.

2.1.4. Setup of the virtual field MR facility: rhizotube geometry and placement

The placement of the rhizotubes was chosen according to the design of the field MR system in Selhausen, as described in Cai et al. (2016): Rhizotubes with an outer diameter of 6.4 cm were inserted horizontally into the soil at six different depth levels (10, 20, 40, 60, 80 and 120 cm) perpendicular to the plant rows. To avoid the effects of the upper rhizotubes on the root observations in the deeper rhizotubes, the rhizotubes were shifted horizontally by 10 cm at each depth level. A sketch of the virtual field plot with maize root systems and rhizotubes is shown in Fig. 1(a and b).

2.1.5. Virtual soil layer sampling and calculation of volumetric root length density

We sampled soil layers of the entire field at 6 different depth levels (5-15, 15-25, 35-45, 55-65, 75-85 and 115-125 cm). To calculate vRLD of our simulated root systems, we cropped the root systems to the soil layers. vRLD was then calculated as the cropped root length divided by the volume of the soil layers and has the unit (cm cm^{-3}).

2.1.6. Virtual MR image sampling procedure, image size and location within the rhizotube and calculation of pRLD

The sampling procedure of virtual MR images was based on the setup described by Lärm et al. (2023) for the minirhizotron facilities in

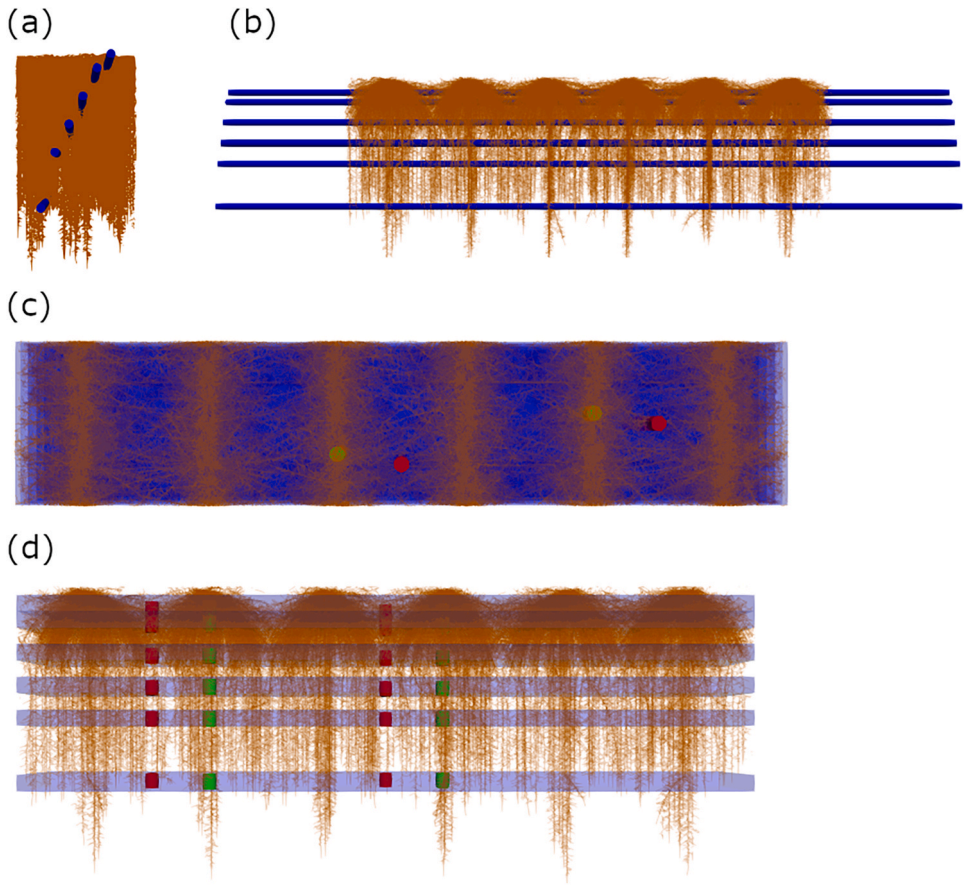

Fig. 1. Virtual field plot with maize root systems (brown) and rhizotubes at six different depth levels (blue): front view in x-direction (a) and front view in y-direction (b); Virtual field plot with maize root systems (brown), soil layers (blue), 2 inter-row soil cores (red) and 2 inter-plant soil cores (green) at six different depth levels: top view (c) and front view in y-direction (d).

Selhausen. Along each rhizotube, 20 image positions were chosen. For maize, the image positions were composed of four groups of five images each. The distance between the groups and between the images within a group was set at 9.3 cm and 10 cm, respectively. For winter wheat, 20 image positions were chosen at distances of 10 cm each. For both maize and winter wheat, the first MR image in a rhizotube was taken at the position of the seed of the first plant. Fig. S3 in the supplementary information shows a visualization of the MR image sampling positions along the rhizotube. The size of the MR images was set to 2×2 cm, which corresponds to the size of the images taken with the camera of the VSI system (Vienna Scientific Instruments GmbH) that was also used in Lärm et al. (2023). At each image position, two images were taken on both sides of the rhizotube by rotating the camera 80° clockwise and counterclockwise with respect to the vertical. Fig. S4 in the supplementary information shows a visualization of the location of the MR images within the rhizotube.

Due to the opacity of the soil, we assumed that only the roots in direct contact with the rhizotube surface would be visible in an MR image. This means that the center line of these roots is at a distance from the rhizotube that is equal to or less than the radius of the root. In CPlantBox, roots are not explicitly simulated as 3D structures, but as line segments to which the root radius is assigned as an attribute. To calculate the pRLD of our simulated root systems, we reduced the root systems to a hollow cylinder around the rhizotube with a thickness set to the maximum root radius. We then cut a volume with the width and length of an MR image at the specified position from this hollow cylinder. We determined the distance to the rhizotube for the two nodes of each root segment within this volume. If the distance to the rhizotube of one or both nodes was less than the root radius, either half or the entire length of the root segment was added to the planar root length. Finally, pRLD (cm cm^{-2}) was calculated by dividing the planar root length by the area of the MR image.

2.2. Geometric properties of the root system

Based on Grabarnik et al. (1998) and van Noordwijk et al. (1985), we described the geometric properties of a plant root system using three types of heterogeneity, namely systematic trends of root distribution, root growth anisotropy, and root clustering. It should be noted that we considered variations in geometric properties only in vertical, but not in horizontal direction, although it can be assumed that horizontal deviations are significant in row crops such as maize. In this study, however, geometric properties were only used to explain variations in pRLD and vRLD, for which we calculated a single value per depth level.

A systematic trend in root distribution describes a variation in root length density at the level of the root system or field and is described in this study using the coefficient of variation of the relative root length density *rRLD*. We thereby defined *rRLD* as the ratio of the root length density of an entire soil layer at a specific depth to the root length density of the entire soil volume and calculated it as

$$rRLD(z) = \frac{RLD(z)}{\int_0^{l_z} RLD(z)dz} \tag{1}$$

where *rRLD* is the relative root length density (cm^{-1}), *RLD* is the root length density of a soil layer at depth z (cm cm^{-3}) and l_z is the depth within which the root length density of the entire soil volume was calculated, which was set to 130 cm. The coefficient of variation *CV* of *rRLD* was then calculated as

$$CV\ of\ rRLD = \frac{SD_{rRLD}}{\overline{rRLD}} \tag{2}$$

where SD_{rRLD} is the standard deviation of *rRLD* across all depths, and $\overline{rRLD}$ is the mean *rRLD* across all depths. The greater *CV* of *rRLD*, the more heterogeneous the distribution of root length density across depth.

Root growth anisotropy describes the non-uniform orientation of roots in the soil. According to Noordwijk (1987), the degree of anisotropy A_n' of roots within a given soil volume can be defined from the number of roots N_a, N_b and N_c intersecting the mutually perpendicular planes A, B, and C, which are oriented in x, y, and z direction.

$$A_n' = \sqrt{\left((N_a - N_m)^2 + (N_b - N_m)^2 + (N_c - N_m)^2\right)/N_m^2} \tag{3}$$

where

$$N_m = (N_a + N_b + N_c)/3 \tag{4}$$

If roots are distributed completely isotropic, $A_n' = 0$. For completely parallel root systems, $A_n' = \sqrt{6}$. A normalized anisotropy factor A_n can therefore be defined as

$$A_n = A_n' \Big/ \sqrt{6} \tag{5}$$

We adopted this approach from Noordwijk (1987) and calculated an anisotropy factor $A_n(z)$ for all axial roots present in a soil layer at a certain depth z. Within each soil layer, we inserted a defined number of planes $A_0 \ldots A_i$, $B_0 \ldots B_i$ and $C_0 \ldots C_i$ in each direction x, y and z. The distance between two parallel planes was set to 5 cm, which proved to be a value small enough to calculate a stable anisotropy factor and large enough to achieve reasonable calculation times. It should be noted that the sum of the areas of all planes in each direction is equal, i.e. $\sum A_0 \ldots A_i = \sum B_0 \ldots B_i = \sum C_0 \ldots C_i$. The greater A_n, the more anisotropic the orientation of axial roots. The coefficient of variation *CV* of A_n was then calculated as

$$CV\ of\ A_n = \frac{SD_{A_n}}{\overline{A_n}} \tag{6}$$

where SD_{A_n} is the standard deviation of A_n across all depths, and $\overline{A_n}$ is the mean A_n across all depths. The greater *CV* of A_n, the more heterogeneous the distribution of root growth anisotropy across depth.

Root clustering describes a preferential grouping of roots in the soil leading to variations in root length density on a scale of a few cubic centimeters and can be characterized by the coefficient of variation of root length density within a defined soil volume (Kohl et al., 2007; Logsdon and Allmaras, 1991). We divided each soil layer at depth z into soil cubes with a volume of $20 \times 20 \times 10$ cm^3. For maize and wheat, this resulted in 108 and 39 soil cubes per soil layer, respectively. The coefficient of variation at depth z, $CV(z)$, was then calculated as

$$CV(z) = \frac{SD_{RLD(sc,z)}}{\overline{RLD(sc,z)}} \tag{7}$$

where $SD_{RLD(sc,z)}$ is the standard deviation of the root length density of all soil cubes within a soil layer at depth z (cm cm^{-3}), and $\overline{RLD(sc,z)}$ is the mean root length density of all soil cubes within a soil layer at depth z (cm cm^{-3}). The higher $CV(z)$, the more root clustering can be expected in a soil layer at depth z. In the following, $CV(z)$ is named $CV_{clustering}(z)$ to distinguish it from *CV of rRLD* and *CV of* A_n. We calculated $CV_{clustering}(z)$ for each depth level of each simulation run.

2.3. Simulation scenarios with different soil sampling schemes, MR image sampling procedures, MR image sizes, rhizotube diameters and plant densities

To analyze the effect of different MR image sampling procedures, MR image sizes, rhizotube diameters, plant densities and soil sampling schemes on the relationship between pRLD and vRLD, we performed additional simulation scenarios in which we varied one of these parameters at a time while keeping the other parameters constant Table 1.

Table 1
Overview of simulation scenarios, the parameter set corresponding to the setup of the field experiment conducted at the minirhizotron facilities in Selhausen in 2021 and 2022 is indicated in bold, the base parameter set from which the parameters were varied one at a time for the different simulation scenarios is indicated in italics.

Parameters	Values/Variables	
	Maize	Winter wheat
Inter- row distance	***75***, 50 cm	***21***, 12 cm
Inter-plant distance	***12***, 20 cm	***1.5***, 3 cm
Plant density	***11***, 10 plants m^{-2}	***317***, 278 plants m^{-2}
Soil sampling scheme	*Soil layer*, Soil cores: (1) 2 mixed soil cores (1 inter-row core, 1 inter-plant core) (2) 2 inter-row soil cores, (3) **2 inter-plant soil cores**, (4) 4 mixed soil cores (2 inter-row cores, 2 inter-plant cores)	
MR image sampling procedure	**Selhausen setup** (20 grouped image positions along the rhizotube), Low-resolution (20 evenly distributed image positions along the rhizotube), High-resolution (40 evenly distributed image positions along the rhizotube), *Continuous* (1 single continuous image along the rhizotube)	
MR image size	***2 × 2 cm***, 6 × 4 cm, entire rhizotube surface	
Outer rhizotube diameter	5.7 cm, ***6.4cm***, 7 cm	

2.3.1. MR image sampling procedure

In addition to the image sampling procedure from the Selhausen setup, we performed a low- and a high-resolution image sampling procedure in which we chose 20 and 40 image positions, respectively, that were evenly distributed along the rhizotube. We also chose a single continuous image position along the rhizotube, which we termed continuous image sampling procedure. In all of these alternative image sampling procedures, the first MR image or the start of continuous image acquisition in a rhizotube was located at the position of the first plant seed minus half the inter-row distance, and the last MR image or the end of continuous image acquisition in a rhizotube was located at the position of the last plant seed plus half the inter-row distance. An overview of all MR image sampling procedures is given in Table 1. A visualization of the MR image sampling positions along the rhizotube in the different MR image sampling procedures can be found in the supplementary information in Fig. S3.

2.3.2. MR image size

Additional simulations were performed using MR images with a size of 6 × 4 cm, corresponding to the size of images captured using the self-built camera system currently employed in the field MR facilities in Selhausen. Just as with the 2 × 2 cm MR images, two images were taken on both sides of the rhizotube by rotating the camera 80° clockwise and counterclockwise relative to the vertical. In addition, we performed simulations using MR images of the entire rhizotube surface. These images correspond to the type of images frequently used in MR studies in the literature (e.g. Arnhold et al. (2024); Liao et al. (2015); Holder et al. (2025)). An overview of the used MR image sizes and their locations within the rhizotube is given in Table 1. An illustration of the locations of the different sized MR images within the rhizotube is given in the supplementary information in Fig. S4.

2.3.3. Outer rhizotube diameter

Additional simulations were performed with two different outer rhizotube diameters: 5.7 cm, corresponding to the rhizotube diameters used in the studies by Black et al. (2017) and Garré et al. (2011), and 7 cm, corresponding to the rhizotube diameters used in the studies by Haarhoff et al. (2021) and Holder et al. (2025). An overview of the used outer rhizotube diameters is given in Table 1.

2.3.4. Plant density

Additional simulations were performed with different plant densities. For maize, the alternative inter-row and inter-plant spacings were set to 50 cm and 20 cm, respectively, resulting in 10 plants per m^2. For winter wheat, the alternative inter-row and inter-plant spacings were set to 12 cm and 3 cm, respectively, resulting in approximately 278 plants per m^2. To simulate these alternative plant densities, we used 8 rows of 6 maize plants and 16 rows of 30 wheat plants, ensuring that the length of each rhizotube was sufficient to remain within the simulated root zone. These alternative plant densities correspond to the usual plant densities applied in Europe (Testa et al., 2016; De Vita et al., 2017). An overview of the used plant densities is given in Table 1.

2.3.5. Soil sampling scheme

In addition to virtual soil layers, we sampled virtual soil cores with a radius of 4.5 cm and a length of 10 cm in 6 different depth levels (5-15, 15-25, 35-45, 55-65, 75-85 and 115-125 cm) using four different sampling schemes: (i) 2 soil cores: 1 inter-row core, 1 inter-plant core, (ii) 2 soil cores: 2 inter-row cores, (iii) 2 soil cores: 2 inter-plant cores, (iv) 4 soil cores: 2 inter-row cores, 2 inter-plant cores. It should be noted that the soil cores were sampled in a virtual field without rhizotubes to exclude the influence of the rhizotubes on the sampled roots. The locations of the soil cores are shown in Fig. 1(c and d). An overview of the soil core sampling schemes is given in Table 1.

2.4. Statistics

Statistical analyses were performed in Python version 3.12.3.

3. Results

3.1. Comparison of experimentally measured and simulated pRLD and vRLD values

To evaluate the plausibility of our simulated pRLD and vRLD values and their relationship with each other, we compared them with experimentally measured values (Fig. 2). A description of the experimental measurement of pRLD and vRLD in the field experiment at the minirhizotron facilities in Selhausen is given in the supplementary information in section S5 and Table S6. The model results were derived from simulations based on the setup of the field experiment at the minirhizotron facilities in Selhausen (Table 1). Here, simulated vRLD was not obtained from virtual soil layers, but from two virtual inter-plant soil cores per soil depth, which had the same size and location as the experimental soil cores. (Fig. 1c and d). For maize, experimentally measured pRLD and vRLD values are within the point cloud of simulation results. For winter wheat, the simulated pRLD values approximately correspond to the experimentally measured values, but the simulated vRLD values mostly underestimate the experimentally measured values. One reason for the discrepancy between the measured and simulated vRLD values may be that only one soil core per depth level was taken for winter wheat, which is clearly insufficient to obtain a good estimate of vRLD in the field. Furthermore, the development of the root system in the field MR facilities, where pRLD was measured, may differ from the development of the root system in the additional field, where soil coring took place to determine vRLD (see supplementary information S5). Another possible reason for the discrepancy is that the simulation model does not consider how the behavior of winter wheat root growth changes when it encounters a rhizotube, e.g. by increased root branching. Nevertheless, both the experiment and the simulation show that pRLD values obtained from MR images are lower than vRLD values determined from soil coring and both pRLD and vRLD values generally decrease with depth. Based on these results, we assume that our simulation model provides plausible estimates of the ground truth values of pRLD and vRLD.

3.2. Relationship between simulated pRLD and vRLD for the setup of the field experiment at the MR facilities in Selhausen

Fig. 3 shows the relationship between simulated pRLD and vRLD

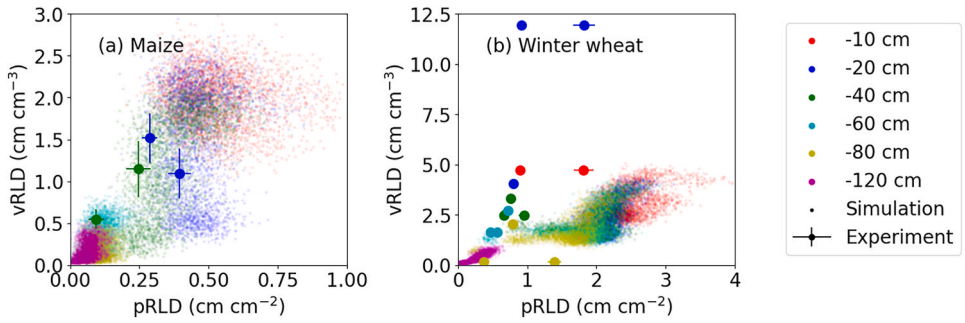

Fig. 2. Experimental and simulated relationships between pRLD and vRLD at different depth levels are shown for maize (a) and winter wheat (b). For the experimental results, n = 4 and 1 for vRLD, and n = 3 and 5 for pRLD at each depth level for maize and winter wheat, respectively; for the simulation results, n = 3200 (100 realizations of root system architecture x 32 parameterizations of axial gravitropism) at each depth level for both maize and winter wheat.

values for different soil depths for maize and winter wheat. As vRLD should be zero when pRLD is zero, we fitted linear regression models with zero intercept to the data points at each depth level. However, the slopes of the regression lines at different depths did not differ greatly from each other, indicating a similar relationship between pRLD and vRLD values at different depth levels. In the upper soil layers down to a depth of −20 cm in maize respectively −40 cm in winter wheat, R^2 values of fitted regression models were negative, indicating that correlations between pRLD and vRLD are extremely weak in the topsoil and that the mean pRLD is a better predictor of vRLD than the regression model. In the subsoil layers, however, R^2 reached values of up to 0.32 in maize and 0.87 in winter wheat, indicating a respectable model fit. Slopes and R^2 of regression models are listed for each depth level and for both maize and winter wheat in Table S7 in the supplementary information. Additionally, we fitted linear regression models with zero intercept at all combined depths and achieved R^2 values of 0.91 and 0.83 for maize and winter wheat, respectively.

3.3. *Influence of geometric properties of the root system on the relationship between pRLD and vRLD*

We analyzed the relationship between the ratio of vRLD to pRLD (*vRLD*/*pRLD*) and the geometric properties of root systems, i.e. systematic trends, root growth anisotropy, and root clustering, in both maize and winter wheat at six different depths (Fig. 4). Higher values of *CV of rRLD* and, consequently, a more heterogeneous distribution of root length density across depth as well as higher values of *CV of* A_n and, consequently, a greater variation in root growth anisotropy across depth led to higher values of *vRLD*/*pRLD* in both maize and winter wheat at all depth levels. Higher values of $CV_{clustering}$ and, consequently, more root clustering led to lower values of *vRLD*/*pRLD* in maize and to higher values of *vRLD*/*pRLD* in winter wheat at all depth levels.

3.4. *Influence of different MR image sampling procedures, MR image sizes, rhizotube diameters, plant densities and soil sampling schemes on the relationship between pRLD and vRLD*

We analyzed the effect of different MR image sampling procedures, MR image sizes, rhizotube diameters and plant densities on the relationship between pRLD and vRLD (Fig. 5). Comparing the relationship between pRLD and vRLD values from the Selhausen setup, the low- and high-resolution, and the continuous image sampling procedures showed that fewer MR images and thus a smaller imaged area resulted in greater dispersion of pRLD values, as the variation in imaged root length was higher. This was evidenced by lower R^2 values and true for both maize and winter wheat. The slopes of the regression lines between the pRLD and vRLD values obtained using low- and high-resolution and continuous image sampling procedures, as well as the Selhausen setup for winter wheat only, were all very similar. However, the slope of the regression line between the pRLD and vRLD values obtained using the Selhausen setup in maize differed (Fig. 5a and b). This shows that the relationship between pRLD and vRLD values can be accurately represented using fewer MR images, provided these images are evenly distributed along the rhizotube. Analysis of different image sizes revealed that the pRLD values of images measuring 2 × 2 cm showed greater variation than the pRLD values of images measuring 6 × 4 cm. The R^2 value of the adjusted linear regression between pRLD and vRLD was therefore lower for images measuring 2 × 2 cm than for images measuring 6 × 4 cm. However, the relationship between the pRLD and vRLD values obtained from MR images measuring 2 × 2 cm and 6 × 4 cm was almost the same, as indicated by the similar slopes of the regression lines. The relationship between the pRLD and vRLD values obtained from MR images of the entire rhizotube surface differed from that obtained from smaller MR images and could not be described as well by a linear regression model with zero intercept, as evidenced by the comparatively lower R^2 values. This is because the relationship between pRLD and vRLD in the upper soil layers differs more from that in the

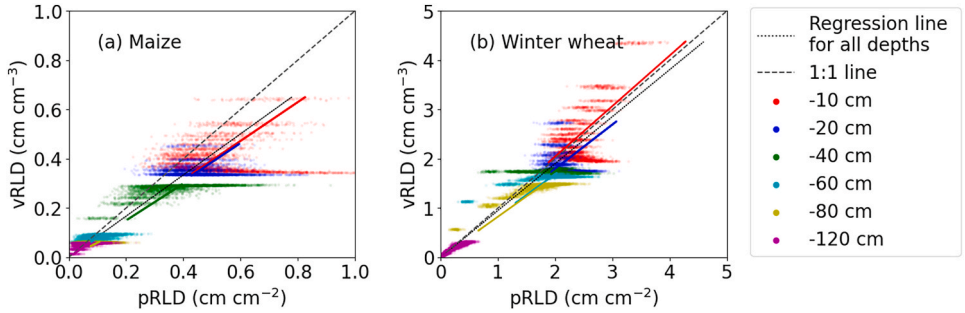

Fig. 3. Relationship between simulated pRLD and vRLD for maize (a) and winter wheat (b) for soil depths between −10 cm and −120 cm. For each soil depth, n = 3200 (100 realizations of root system architecture x 32 parameterizations of axial gravitropism). Regression lines are shown individually for each soil depth in the respective color and in black for all depths combined.

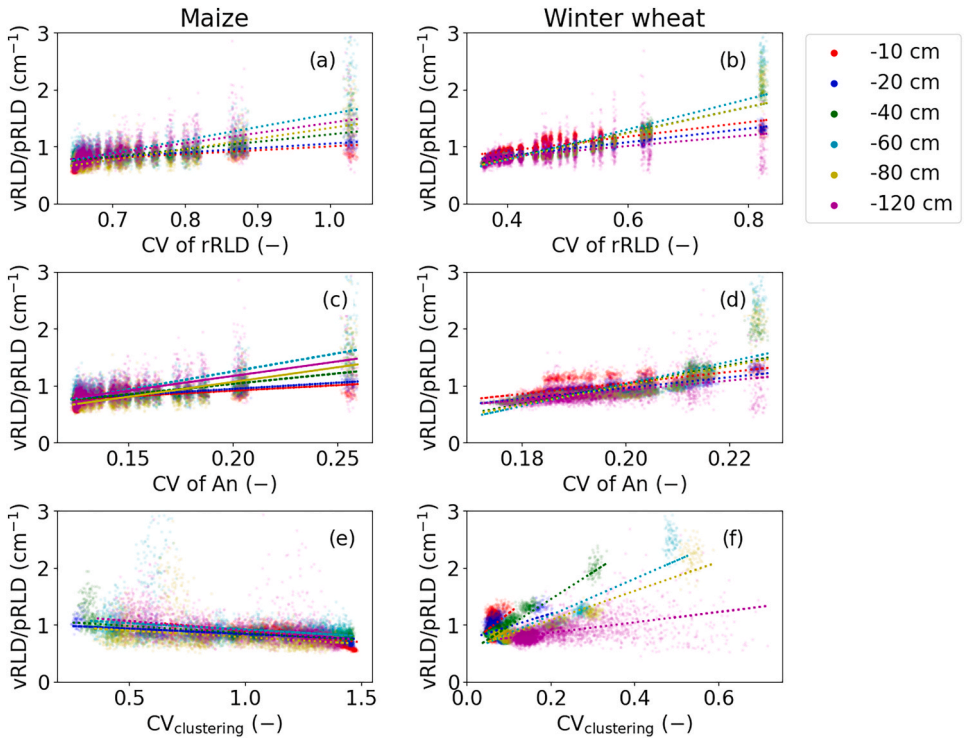

Fig. 4. Relationship between the ratio of vRLD to pRLD and the geometric properties of roots systems, i.e. systematic trends (a, b), root growth anisotropy (c, d) and root clustering (e, d), for maize (a, c, d) and winter wheat (b, d, f) for soil depths between −10 cm and −120 cm. For each soil depth, n = 3200 (100 realizations of root system architecture x 32 parameterizations of axial gravitropism). Regression lines are shown individually for each soil depth.

lower layers in MR images of the entire rhizotube surface than in smaller MR images taken at the sides of the rhizotubes (c.f. Fig. 3 and Fig. S8 in the supplementary information). These findings were true for both maize and winter wheat (Fig. 5c and d). Larger rhizotube diameters led to lower ratios of vRLD to pRLD, which was true for both maize and winter wheat. This can be explained by the fact that more roots encounter a rhizotube with a large diameter and grow along it before bending back into the bulk soil than is the case for a rhizotube with a small diameter. In this way, MR images taken in a rhizotube with a large diameter capture more roots than those taken in a rhizotube with a small diameter and pRLD values are thus higher (Fig. 5e and f). Different plant densities did not lead to a different relationship between pRLD and vRLD, which was true for both maize and winter wheat (Fig. 5g and h). Different virtual soil sampling schemes led to different vRLD values and thus to different relationships between pRLD and vRLD: In maize, 2 inter-plant as well as 2 or 4 mixed soil cores largely overestimated vRLD, while 2 inter-row soil cores underestimated vRLD as compared to soil layer vRLD. In winter wheat, vRLD measured using 2 and 4 mixed soil cores corresponded well with soil layer vRLD. However, vRLD was once again overestimated using 2 inter-plant soil cores and underestimated using 2 inter-row soil cores. As expected, the correlations between pRLD and vRLD were weak for vRLD from inter-row soil cores and strong for vRLD from soil layers. However, strong correlations were also observed for vRLD from 2 to 4 mixed soil cores, as well as from inter-plant soil cores.

4. Discussion

4.1. Using model simulation to complement experimental minirhizotron studies

Model simulation is a valuable tool for complementing experimental minirhizotron studies, as it provides a better understanding of the factors influencing pRLD observed in minirhizotron images, and its relationship with vRLD. Thirty years ago, (Pagès et al., 1997) used model simulation to examine the part of a virtual root system that lies geometrically within a virtual rhizotube and showed that minirhizotron observations underestimate maximum rooting depth. Since then, root architecture models have been developed to such an extent that we are now able to explicitly simulate root growth around rhizotubes in a realistic way and to capture virtual MR images at a defined position along the rhizotube.

One question that remains unresolved is the definition of the distance from the surface of the rhizotube into the soil at which roots can be detected on MR images, known as the “depth of view.” In this study, it was assumed that only roots in direct contact with the rhizotube surface would be visible on an MR image. However, this is a conservative assumption and may lead to an underestimation of pRLD since it could be speculated that a root might also be visible on an MR image if there is a thin layer of soil between the root and the surface of the rhizotube. However, given the opacity of the soil, we considered this assumption to be more plausible than the approach taken in previous studies, which assumed arbitrary values for the depth of view between 1 mm and 3 mm (Sanders and Brown 1978; Cai et al., 2018; Liao et al., 2015; Garré et al., 2011; Morandage et al., 2019). Taylor et al. (2014) calculated a depth of view of 0.78 mm using root diameters measured in the field and those visible on MR images. However, this calculation is based on the assumption that observed and actual root diameters only differ when the actual root radius is greater than the depth of view. Since only a few of the roots they examined and excavated had a radius greater than 0.78 mm, the R^2 value of their fitting was very low at $R^2 = 0.43$, which makes us doubt the general validity of their specified depth-of-view value. Upchurch (1987) and Sullivan and Welker (2005) have suggested that the depth of view may vary depending on soil type, but there is currently no evidence to support this assumption.

Comparing the simulated and experimentally measured pRLD and vRLD values in this study showed that our simulations largely underestimated the experimentally measured vRLD values for winter wheat.

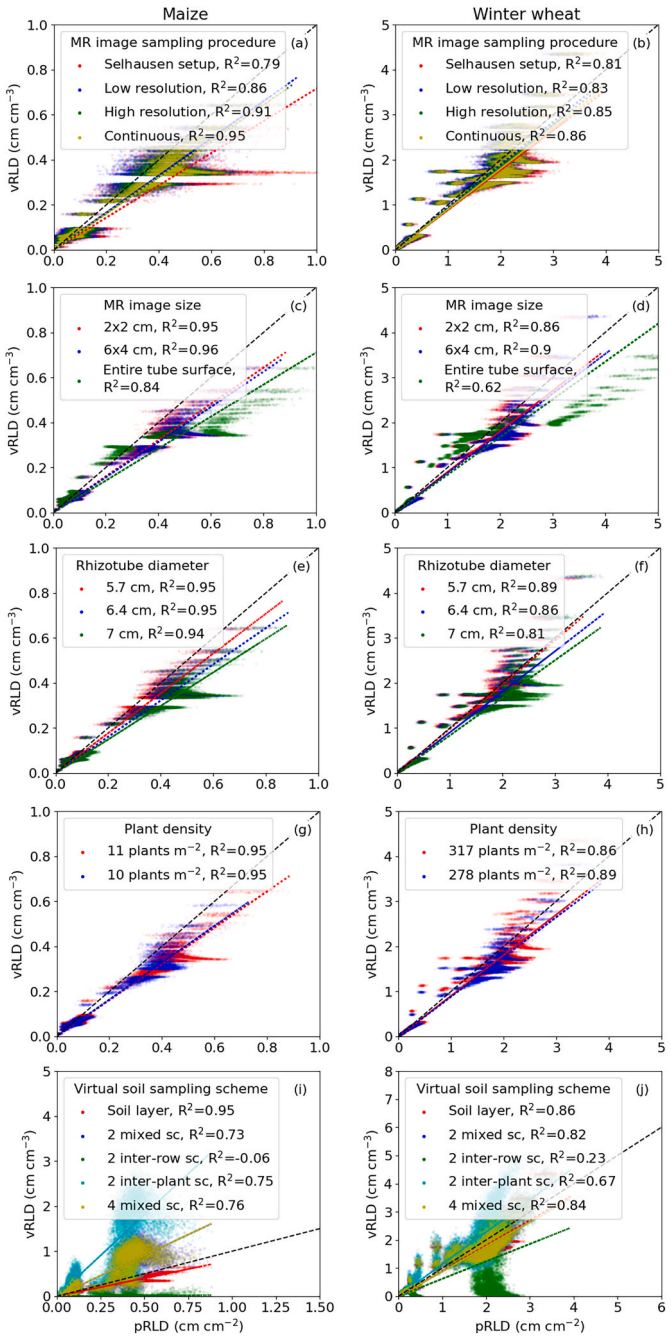

Fig. 5. Influence of MR image sampling procedure (a, b), MR image size (c, d), rhizotube diameter (e, f), plant density (g, h) and virtual soil sampling scheme where sc stands for soil cores (i, j) on the relationship between pRLD and vRLD for maize (a, c, e, g, i) and winter wheat (b, d, f, h, j). For each scenario, n = 19200 (100 realizations of root system architecture x 32 parameterizations of axial gravitropism x 6 depths). The black dashed line represents the 1:1 line. Linear trend lines with zero intercept are shown for each scenario in dashed lines in the respective colors.

In addition to the insufficient number of soil cores and soil core measurements in a field different to the one in which MR measurements were taken, one possible reason for this inconsistency is an inaccurate simulation of winter wheat roots around the rhizotubes. Although rhizotubes are expected to influence root growth and root branching rate (Wacker et al., 2024), the precise way in which they impact these factors remains unclear and is therefore not incorporated into CPlantBox or in any other root architecture model. More experimental research is needed here, and the findings could be used to create growth rules for root architecture models. This would enable a more realistic simulation of root growth in MR systems, as well as a better reproduction of real MR systems in the field.

4.2. *Relationship between pRLD and vRLD*

Our simulations showed that correlations between pRLD and vRLD were weak in the topsoil and strong in the subsoil. Weak correlations between pRLD and vRLD in the topsoil have also been reported in many experimental studies (Arnhold et al., 2024; Box Jr. and Ramsuer, 1993; Ephrath et al., 1999; Heeraman and Juma, 1993; Kage et al., 2000; Samson and Sinclair, 1994; Vos and Groenwold, 1987; Machado and Oliveira, 2003). In these studies, weak correlations between pRLD and vRLD were explained by several factors, including air gaps between soil and rhizotube due to soil drying, light penetration into the rhizotube or physical disturbances through the rhizotubes during installation (Arnhold et al., 2024; Kage et al., 2000; Heeraman and Juma, 1993). Our simulation results suggest that the mere fact that root systems originate from a seed and that root distribution is therefore more heterogeneous in the topsoil is a key factor leading to such weak correlations between pRLD and vRLD in the topsoil. Our simulations also showed that the ratio of vRLD to pRLD in the subsoil remained relatively constant across depth, which has also been shown experimentally by Arnhold et al. (2024) for winter wheat. This implies that pRLD can be used to describe relative root length density in the field for both row-crops such as maize and non-row crops such as winter wheat.

An analysis of the geometric properties of the root system showed that root systems with high heterogeneity in root length density distribution or in root growth anisotropy across depth have higher ratios of vRLD to pRLD. These results are consistent with the observations of (Bublitz et al., 2022), who found that large variations in root length density across depth lead to poor agreement between root length density measurements using the profile wall method, which measures planar root length density, and the soil monolith method, which measures volumetric root length density. Our study further showed that root clustering led to lower ratios of vRLD to pRLD in maize, and to higher ratios of vRLD to pRLD in winter wheat. This contrasting effect of root clustering on the ratio of vRLD to pRLD in different plant species can be attributed, on the one hand, to the inter-row and inter-plant spacing chosen for each species (Logsdon and Allmaras, 1991) and, on the other hand, to the size of the soil cubes, both of which influence the coefficient of variation of root length density, which we used to characterize root clustering. Therefore, we conclude that root clustering is likely to affect the relationship between vRLD and pRLD, but the exact effect depends on the scale at which root clustering is considered, as well as on the inter-row and inter-plant distances chosen.

Our simulations showed that the mean pRLD values obtained from MR images distributed evenly along the rhizotube were similar to those obtained from continuous MR images, but different to those obtained from grouped MR images. These findings correspond to observations of Dubach and Russelle (1995) in an experimental field study with horizontal rhizotubes, who found that using only every second MR image did not affect the accuracy of pRLD, whereas accuracy decreased when only the first half of the MR images were used. This suggests that recording continuous MR images along the entire length of the rhizotubes, as proposed by Lärm et al. (2024), is not necessary to obtain accurate pRLD values, but that the MR images should be evenly distributed along the rhizotube.

Our simulations showed that larger rhizotube diameters resulted in a lower vRLD-to-pRLD ratio and that MR scans of the entire rhizotube surface revealed a different relationship between pRLD and vRLD compared to MR images of smaller sections of the rhizotube. This suggests that a simple conversion approach from pRLD to vRLD, which is independent of MR specifications and has been used in many literature studies (Holder et al., 2025; Sanders and Brown, 1978; Haarhoff et al., 2021; Garré et al., 2011; Cai et al., 2018; Liao et al., 2015; Geng et al.,

2023) will not produce reliable vRLD values. Simulations with vRLD derived from differently placed soil cores as well as from soil layers showed that soil core vRLD differed strongly from soil layer vRLD for the row-crop maize and less strong for the non-row crop winter wheat, which is consistent with findings in the literature (Buczko et al., 2009; Wu et al., 2017; Morandage et al., 2019). Simulations showed that the vRLD of two to four mixed soil cores was in good agreement with the actual vRLD of soil layers for the non-row crop winter wheat, which has a high plant density and relatively homogeneous horizontal root distribution. However, this was not the case for the row-crop maize, which has a low plant density and heterogeneous horizontal root distribution. When experimentally determining the relationship between pRLD and vRLD, this discrepancy in vRLD from soil cores and soil layers must be considered. The simulated R^2 values of around 0.7 between pRLD and vRLD, as obtained from mixed and inter-plant soil cores, are consistent with the R^2 values for winter wheat, as experimentally determined and reported by Arnhold et al. (2024).

Model availability

The CPlantBox code used to run the simulations, the simulation results, and the code used to plot these results as well as the code for the simulation experiment based on the study by Yao et al. (2024) are all available at https://github.com/Plant-Root-Soil-Interactions-Modelling/CPlantBox/tree/prld_vrld/tutorial/prld_vrld.

CRediT authorship contribution statement

Magdalena Landl: Conceptualization, Data curation, Formal analysis, Methodology, Software, Visualization, Writing – original draft, Writing – review & editing. **Sibghat Ullah:** Conceptualization, Methodology, Software. **Lena Lärm:** Data curation, Writing – review & editing. **Anja Klotzsche:** Writing – review & editing. **Jan Vanderborght:** Conceptualization, Supervision, Writing – review & editing. **Andrea Schnepf:** Conceptualization, Funding acquisition, Methodology, Supervision, Writing – review & editing.

Declaration of competing interest

The authors declare that they have no known competing financial interests or personal relationships that could have appeared to influence the work reported in this paper.

Acknowledgements

This work was funded by the German Research Foundation (DFG) as part of the Priority Program 2089 (grant 403641034), the German Federal Ministry of Education and Research (BMBF) as part of the "RhizoWheat" project (grant 031B1413B) within the "Rhizo4Bio (Phase 2)" funding initiative, and the German Research Foundation (DFG) as part of Germany's Excellence Strategy (grant EXC-2070—390732324—PhenoRob).

Appendix A. Supplementary data

Supplementary data to this article can be found online at https://doi.org/10.1016/j.rhisph.2026.101294.

Data availability

Data will be made available on request.

References

Arnhold, J., Ispizua Yamati, F.R., Kage, H., Mahlein, A.-K., Koch, H.-J., Grunwald, D., 2024. Minirhizotron measurements can supplement deep soil coring to evaluate root growth of winter wheat when certain pitfalls are avoided. Plant Methods 20 (1), 183. https://doi.org/10.1186/s13007-024-01313-0.

Baldwin, J., Tinker, P., Marriott, F., 1971. The measurement of length and distribution of onion roots in the field and the laboratory. J. Appl. Ecol. 543–554. https://doi.org/10.2307/2402890.

Bauer, F.M., Lärm, L., Morandage, S., Lobet, G., Vanderborght, J., Vereecken, H., Schnepf, A., 2022. Development and validation of a deep learning based automated minirhizotron image analysis pipeline. Plant Phenomics 2022. https://doi.org/10.34133/2022/9758532.

Bengough, A.G., Castrignano, A., Pagès, L., van Noordwijk, M., 2000. Sampling strategies, scaling, and statistics. In: Smit, A.L., Bengough, A.G., Engels, C., van Noordwijk, M., Pellerin, S., van de Geijn, S.C. (Eds.), Root Methods: a Handbook. Springer, Berlin Heidelberg, Berlin, Heidelberg, pp. 147–173. https://doi.org/10.1007/978-3-662-04188-8_5.

Bernier, P.Y., Robitaille, G., 2004. A plane intersect method for estimating fine root productivity of trees from minirhizotron images. Plant Soil 265 (1), 165–173. https://doi.org/10.1007/s11104-005-0056-y.

Black, C.K., Masters, M.D., LeBauer, D.S., Anderson-Teixeira, K.J., DeLucia, E.H., 2017. Root volume distribution of maturing perennial grasses revealed by correcting for minirhizotron surface effects. Plant Soil 419 (1), 391–404. https://doi.org/10.1007/s11104-017-3333-7.

Box, Jr.JE., Ramsuer, E.L., 1993. Minirhizotron wheat root data: comparisons to soil core root data. Agron. J. 85 (5), 1058–1060. https://doi.org/10.2134/agronj1993.00021962008500050019x.

Böske, L.N., Falge, E., Liedtke, M., Böttcher, C., Iwers-Braden, D., Meisner, H., Herbst, M., 2025. Applying minirhizotrons to observe spatiotemporal variations in rooting depth and distribution in agroecosystems to improve the performance of hydrological models. Vadose Zone J. 24 (1), e20382. https://doi.org/10.1002/vzj2.20382.

Bublitz, T.A., Kemper, R., Müller, P., Kautz, T., Döring, T.F., Athmann, M., 2022. Relating profile wall root-length density estimates to monolith root-length density measurements of cover crops. Agronomy 12 (1), 48.

Buczko, U., Kuchenbuch, R.O., Gerke, H.H., 2009. Evaluation of a core sampling scheme to characterize root length density of maize. Plant Soil 316 (1), 205–215. https://doi.org/10.1007/s11104-008-9771-5.

Cai, G., Vanderborght, J., Couvreur, V., Mboh, C.M., Vereecken, H., 2018. Parameterization of root water uptake models considering dynamic root distributions and water uptake compensation. Vadose Zone J. 17 (1). https://doi.org/10.2136/vzj2016.12.0125.

Cai, G., Vanderborght, J., Klotzsche, A., van der Kruk, J., Neumann, J., Hermes, N., Vereecken, H., 2016. Construction of minirhizotron facilities for investigating root zone processes. Vadose Zone J. 15 (9). https://doi.org/10.2136/vzj2016.05.0043 vzj2016.2005.0043.

De Vita, P., Colecchia, S.A., Pecorella, I., Saia, S., 2017. Reduced inter-row distance improves yield and competition against weeds in a semi-dwarf durum wheat variety. Eur. J. Agron. 85, 69–77. https://doi.org/10.1016/j.eja.2017.02.003.

Dubach, M., Russelle, M.P., 1995. Reducing the cost of estimating root turnover with horizontally installed minirhizotrons. Agron. J. 87 (2), 258–263. https://doi.org/10.2134/agronj1995.00021962008700020019x.

Ephrath, J.E., Silberbush, M., Berliner, P.R., 1999. Calibration of minirhizotron readings against root length density data obtained from soil cores. Plant Soil 209 (2), 201–208. https://doi.org/10.1023/A:1004556100253.

Garré, S., Javaux, M., Vanderborght, J., Pages, L., Vereecken, H., 2011. Three-dimensional electrical resistivity tomography to monitor root zone water DynamicsAll rights reserved. No part of this periodical may be reproduced or transmitted in any form or by any means, electronic or mechanical, including photocopying, recording, or any information storage and retrieval system, without permission in writing from the publisher. Vadose Zone J. 10 (1), 412–424. https://doi.org/10.2136/vzj2010.0079.

Geng, L., Li, L., Sheng, W., Sun, Q., Yang, J., Huang, Q., Lv, P., 2023. Compound minirhizotron device for root phenotype and water content near root zone. Comput. Electron. Agric. 205, 107592. https://doi.org/10.1016/j.compag.2022.107592.

Giraud, M., Gall, S.L., Harings, M., Javaux, M., Leitner, D., Meunier, F., Rothfuss, Y., van Dusschoten, D., Vanderborght, J., Vereecken, H., Lobet, G., Schnepf, A., 2023. CPlantBox: a fully coupled modelling platform for the water and carbon fluxes in the soil–plant–atmosphere continuum. silico Plants 5 (2). https://doi.org/10.1093/insilicoplants/diad009.

Grabarnik, P., Pagès, L., Bengough, A.G., 1998. Geometrical properties of simulated maize root systems: consequences for length density and intersection density. Plant Soil 200 (2), 157–167. https://doi.org/10.1023/A:1004382531671.

Haarhoff, S.J., Lötze, E., Swanepoel, P.A., 2021. Rainfed maize root morphology in response to plant population under no-tillage. Agron. J. 113 (1), 75–87. https://doi.org/10.1002/agj2.20441.

Heeraman, D.A., Juma, N.G., 1993. A comparison of minirhizotron, core and monolith methods for quantifying barley (Hordeum vulgare L.) and fababean (Vicia faba L.) root distribution. Plant Soil 148 (1), 29–41. https://doi.org/10.1007/BF02185382.

Holder, A.J., Robson, P., McCalmont, J.P., 2025. Effect of tillage method on early root growth of miscanthus. Annals of Applied Biology n/a (n/a). https://doi.org/10.1111/aab.70006.

Johnson, M.G., Tingey, D.T., Phillips, D.L., Storm, M.J., 2001. Advancing fine root research with minirhizotrons. Environ. Exp. Bot. 45 (3), 263–289. https://doi.org/10.1016/S0098-8472(01)00077-6.

Kage, H., Kochler, M., Stützel, H., 2000. Root growth of cauliflower (Brassica oleracea L. botrytis) under unstressed conditions: measurement and modelling. Plant Soil 223 (1), 133–147. https://doi.org/10.1023/A:1004866823128.

Khoroshevsky, F., Zhou, K., Bar-Hillel, A., Hadar, O., Rachmilevitch, S., Ephrath, J.E., Lazarovitch, N., Edan, Y., 2024. A CNN-Based framework for estimation of root

length, diameter, and color from in situ minirhizotron images. Comput. Electron. Agric. 227, 109457. https://doi.org/10.1016/j.compag.2024.109457.
Kohl, M., Böttcher, U., Kage, H., 2007. Comparing different approaches to calculate the effects of heterogeneous root distribution on nutrient uptake: a case study on subsoil nitrate uptake by a barley root system. Plant Soil 298 (1), 145–159. https://doi.org/10.1007/s11104-007-9347-9.
Lang, A., Melhuish, F., 1970. Lengths and diameters of plant roots in non-random populations by analysis of plane surfaces. Biometrics 421–431. https://doi.org/10.2307/2529099.
Lee, H.-J., Kim, H.-S., Park, J.M., Cho, H.S., Jeon, J.H., 2020. PIN-mediated polar auxin transport facilitates root−obstacle avoidance. New Phytol. 225 (3), 1285–1296. https://doi.org/10.1111/nph.16076.
Liao, R., Yueming, B., Hong, L., Shunqing, A., Sanxue, R., Yujing, C., Zhangyan, L., Jianli, L., Liu, J., 2015. Root growth of maize as studied with minirhizotrons and monolith methods. Arch. Agron Soil Sci. 61 (10), 1343–1356. https://doi.org/10.1080/03650340.2014.1003812.
Logsdon, S.D., Allmaras, R.R., 1991. Maize and soybean root clustering as indicated by root mapping. Plant Soil 131 (2), 169–176. https://doi.org/10.1007/BF00009446.
Lärm, L., Bauer, F.M., Hermes, N., van der Kruk, J., Vereecken, H., Vanderborght, J., Nguyen, T.H., Lopez, G., Seidel, S.J., Ewert, F., Schnepf, A., Klotzsche, A., 2023. Multi-year belowground data of minirhizotron facilities in selhausen. Sci. Data 10 (1), 672. https://doi.org/10.1038/s41597-023-02570-9.
Lärm, L., Bauer, F.M., van der Kruk, J., Vanderborght, J., Morandage, S., Vereecken, H., Schnepf, A., Klotzsche, A., 2024. Linking horizontal crosshole GPR variability with root image information for maize crops. Vadose Zone J. 23 (1), e20293. https://doi.org/10.1002/vzj2.20293.
Machado, R.M.A., Oliveira, MdRG., 2003. Comparison of tomato root distributions by minirhizotron and destructive sampling. Plant Soil 255 (1), 375–385. https://doi.org/10.1023/A:1026198919074.
Massa, G.D., Gilroy, S., 2003. Touch modulates gravity sensing to regulate the growth of primary roots of Arabidopsis thaliana. Plant J. 33 (3), 435–445. https://doi.org/10.1046/j.1365-313X.2003.01637.x.
Monshausen, G.B., Gilroy, S., 2009. The exploring Root—root growth responses to local environmental conditions. Curr. Opin. Plant Biol. 12 (6), 766–772. https://doi.org/10.1016/j.pbi.2009.08.002.
Morandage, S., Schnepf, A., Leitner, D., Javaux, M., Vereecken, H., Vanderborght, J., 2019. Parameter sensitivity analysis of a root system architecture model based on virtual field sampling. Plant Soil 438 (1), 101–126. https://doi.org/10.1007/s11104-019-03993-3.
Morandage, S., Vanderborght, J., Zörner, M., Cai, G., Leitner, D., Vereecken, H., Schnepf, A., 2021. Root architecture development in stony soils. Vadose Zone J. 20 (4), e20133. https://doi.org/10.1002/vzj2.20133.
Morris, E.C., Griffiths, M., Golebiowska, A., Mairhofer, S., Burr-Hersey, J., Goh, T., von Wangenheim, D., Atkinson, B., Sturrock, C.J., Lynch, J.P., Vissenberg, K., Ritz, K., Wells, D.M., Mooney, S.J., Bennett, M.J., 2017. Shaping 3D root system architecture. Curr. Biol. 27 (17), R919–R930. https://doi.org/10.1016/j.cub.2017.06.043.
Noordwijk, Mv, 1987. Methods for Quantification of Root Distribution Pattern and Root Dynamics in the Field.
Pagès, L., Bengough, G., Anthony, 1997. Modelling minirhizotron observations to test experimental procedures. Plant Soil 189 (1), 81–89. https://doi.org/10.1023/A:1004288430467.
Postma, J.A., Lynch, J.P., 2011. Root cortical aerenchyma enhances the growth of maize on soils with suboptimal availability of nitrogen. Phosphorus, and Potassium Plant Physiology 156 (3), 1190–1201. https://doi.org/10.1104/pp.111.175489.
Rytter, R.-M., Rytter, L., 2012. Quantitative estimates of root densities at minirhizotrons differ from those in the bulk soil. Plant Soil 350 (1), 205–220. https://doi.org/10.1007/s11104-011-0896-6.
Samson, B.K., Sinclair, T.R., 1994. Soil core and minirhizotron comparison for the determination of root length density. Plant Soil 161 (2), 225–232. https://doi.org/10.1007/BF00046393.
Sanders, J.L., Brown, D.A., 1978. A new fiber optic technique for measuring root growth of soybeans under field conditions. Agron. J. 70 (6), 1073–1076. https://doi.org/10.2134/agronj1978.00021962007000060043x.
Schnepf, A., Leitner, D., Landl, M., Lobet, G., Mai, T.H., Morandage, S., Sheng, C., Zörner, M., Vanderborght, J., Vereecken, H., 2018. CRootBox: a structural–functional modelling framework for root systems. Ann. Bot. 121 (5), 1033–1053. https://doi.org/10.1093/aob/mcx221.
Smith, A.G., Petersen, J., Selvan, R., Rasmussen, C.R., 2020. Segmentation of roots in soil with U-Net. Plant Methods 16 (1), 13. https://doi.org/10.1186/s13007-020-0563-0.
Sullivan, P.F., Welker, J.M., 2005. Warming chambers stimulate early season growth of an arctic sedge: results of a minirhizotron field study. Oecologia 142 (4), 616–626. https://doi.org/10.1007/s00442-004-1764-3.
Tardieu, F., 1988. Analysis of the spatial variability of maize root density. Plant Soil 107 (2), 267–272. https://doi.org/10.1007/BF02370556.
Taylor, B.N., Beidler, K.V., Strand, A.E., Pritchard, S.G., 2014. Improved scaling of minirhizotron data using an empirically-derived depth of field and correcting for the underestimation of root diameters. Plant Soil 374 (1), 941–948. https://doi.org/10.1007/s11104-013-1930-7.
Testa, G., Reyneri, A., Blandino, M., 2016. Maize grain yield enhancement through high plant density cultivation with different inter-row and intra-row spacings. Eur. J. Agron. 72, 28–37. https://doi.org/10.1016/j.eja.2015.09.006.
Upchurch, D.R., 1987. Conversion of minirhizotron-root intersections to root length density. In: Minirhizotron Observation Tubes: Methods and Applications for Measuring Rhizosphere Dynamics, pp. 51–65. https://doi.org/10.2134/asaspecpub50.c5.
van Noordwijk, M., Floris, J., de Jager, A., 1985. Sampling schemes for estimating root density distribution in cropped fields. Neth. J. Agric. Sci. 33 (3), 241–261.
Vos, J., Groenwold, J., 1987. The relation between root growth along observation tubes and in bulk soil. In: Minirhizotron Observation Tubes: Methods and Applications for Measuring Rhizosphere Dynamics, pp. 39–49. https://doi.org/10.2134/asaspecpub50.c4.
Wacker, T.S., van der Bom, F., Delory, B.M., Vetterlein, D., Postma, J.A., Nagel, K.A., Schnepf, A., Dresbøll, D.B., 2024. Back to the roots: standardizing root length density terminology. Plant Soil. https://doi.org/10.1007/s11104-024-07075-x.
Wu, Q., Wu, J., Zheng, B., Guo, Y., 2017. Optimizing soil-coring strategies to quantify root-length-density distribution in field-grown maize: virtual coring trials using 3-D root architecture models. Ann. Bot. 121 (5), 809–819. https://doi.org/10.1093/aob/mcx117.
Yao, J., Barés, J., Dupuy, L.X., Kolb, E., 2024. Physical obstacles in the substrate cause maize root growth trajectories to switch from vertical to oblique. J. Exp. Bot. 76 (2), 546–561. https://doi.org/10.1093/jxb/erae378.